ANALYSIS OF BEAM TRANSVERSE INSTABILITIES AT FERMILAB

T. Zolkin*, The University of Chicago, Chicago, IL 60637, USA

Abstract

The transverse beam dynamics in Fermilab Recycler ring has been analyzed using *SCHARGEV* Vlasov solver. In the first part of paper we discuss how *SCHARGEV* analyses collective instabilities for Gaussian bunch with strong space charge in resistive impedance environment. In the second part the bunched beam dynamics is studied depending on head-tail phase and damper gain. An example for Fermilab Recycler is presented.

SSC THEORY AND BUROV EQUATION

For transverse oscillations of bunched beams, a parameter of the space charge strength is a ratio of the maximal space charge tune shift to the synchrotron tune. When this parameter is large, the transverse oscillations are described by a one-dimensional integro-differential **Burov equation**

$$\nu\, y + \frac{1}{Q_{\text{eff}}} \frac{\mathrm{d}}{\mathrm{d}\tau}\left(u^2 \frac{\mathrm{d}\,y}{\mathrm{d}\tau}\right) = \varkappa\, N\left(\hat{W} + \hat{D}\right), \quad \frac{\mathrm{d}\,y}{\mathrm{d}\tau}\bigg|_{\tau \to \pm\infty} = 0,$$

derived in [1]. *SCHARGEV* Vlasov solver is based on numerical solution of the equation above and for more details see [2].

Below we will consider the case of Gaussian bunch which corresponds to a thermal equilibrium when the bunch length is much shorter than the rf wavelength [3]. In this case the Sturm-Liouville problem for no-wake case leads to the **Burov-Balbekov functions** [1,4]:

$$\begin{cases} \bar{y}''(\tau) + \nu\, e^{-\tau^2/2}\, \bar{y}(\tau) = 0, \\ \bar{y}'(\pm\infty) = 0, \end{cases}$$

where the natural system of units is employed: the distance τ is measured in units of the RMS bunch length σ, and, eigenvalues ν_k is measured in units of $u^2/\sigma^2 Q_{\text{eff}}(0) = Q_s^2/Q_{\text{eff}}(0)$. First eight eigenfunctions, $\bar{y}_k(\tau)$, are plotted in Fig. 1.
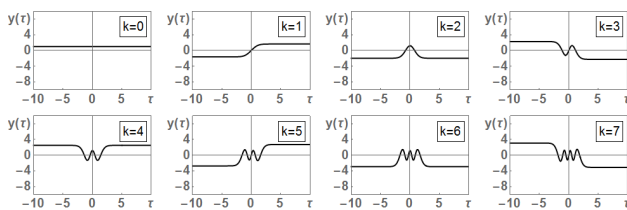
Figure 1: The first 8 eigenfunctions of the Gaussian bunch, $\bar{y}_k(\tau)$. The modes do not depend on the chromaticity, except the common head-tail phase factor $\exp(-i\zeta\tau)$.

* zolkin@uchicago.edu

DIPOLE MOMENTS AND DAMPER

For further discussion we need to introduce the bunch dipole moments defined as functions of the head-tail phase:

$$I_k(\zeta) = \int_{-\infty}^{\infty} \rho(\tau)\bar{y}_k(\tau)e^{i\zeta\tau}\,\mathrm{d}\tau: \quad I_k^*(\zeta) = (-1)^k I_k(\zeta),$$

where $\rho(\tau) = \int_{-\infty}^{\infty} f(v,\tau)\,\mathrm{d}v = (2\pi)^{-1/2} \exp(-\tau^2/2)$ is the normalized line density of the beam. First four of them are plotted in Fig. 2.
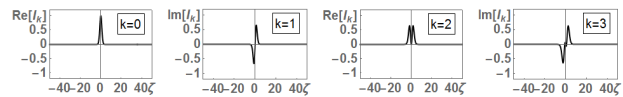
Figure 2: The first 4 bunch dipole moments for the Gaussian bunch as a function of the head-tail phase, $I_k(\zeta)$. Only real or imaginary part is plotted for even and odd ks respectively.

Matrix elements of an operator of the linear bunch by bunch damper can be constructed as a direct product of a set of dipole moment functions

$$\hat{G}_{lm}(\zeta) = \int_{-\infty}^{\infty}\int_{-\infty}^{\infty} \rho(\tau)\rho(\sigma)\bar{y}_l(\tau)\bar{y}_m(\sigma)e^{i\zeta(\tau-\sigma)}\,\mathrm{d}\sigma\,\mathrm{d}\tau$$
$$= I_l(\zeta)I_m^*(\zeta) = (-1)^m I_l(\zeta)I_m(\zeta),$$

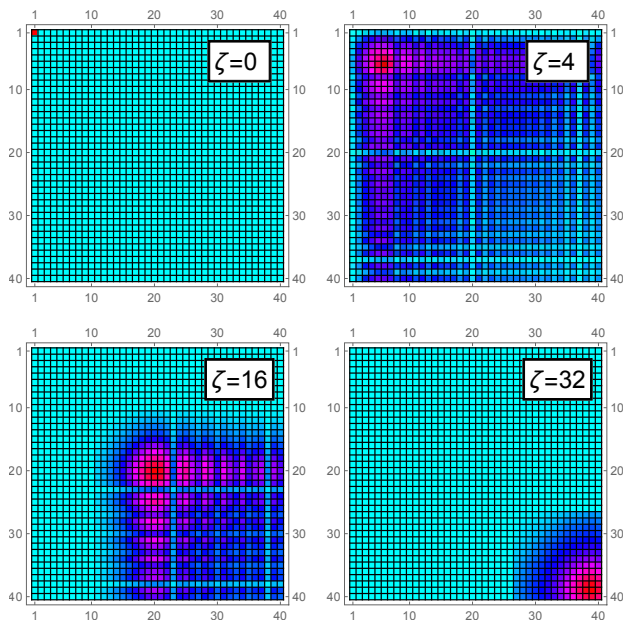(same matrix describes the couple bunch wake terms for sufficiently separated bunches).

Figure 3: Absolute value of 40 by 40 dipole moments direct product matrices, $\hat{G}_{lm}$, plotted for different values of the head-tail phase ($\zeta = 0, 4, 16, 32$).
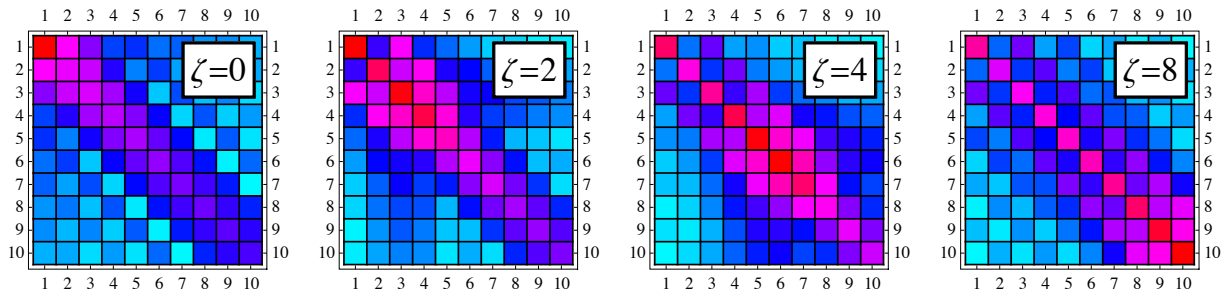
Figure 4: Absolute value of 10 by 10 driving resistive wall wake matrices, $\hat{W}_{lm}$, plotted for different values of head-tail phase ($\zeta = 0, 2, 4, 8$).

WAKE FORCES

When the wake terms $Q_w \gg Q_s^2/Q_{\max}$, the no-wake eigensystem $\{\bar{y}_k(\tau), \nu_k\}$ is strongly perturbed. Below we will provide the results of matrix elements calculation for the resistive wall impedance with wake function $W_1(\tau)$ defined over a distance L as

$$W_m(z < 0) = \frac{2 J_{\mathrm{vc}}}{\pi \, b^{2m+1}(1 + \delta_{m0})} \sqrt{\frac{c}{\sigma_s}} \frac{L}{\sqrt{|z|}},$$

where b is a vacuum chamber radius. The Yokoya factor, J_{vc}, is equal to 1 for round vacuum chamber, and, $\pi^2/24$ and $\pi^2/12$ for horizontal and vertical directions for a flat chamber.

Driving Wake

The matrix elements of the driving (dipole) wake operator in no-wake modes basis are determined as

$$\hat{W}_{lm} = \int_{-\infty}^{\infty} \int_{\tau}^{\infty} \mathrm{d}\sigma \, \mathrm{d}\tau$$
$$W(\tau - \sigma)\rho(\tau)\rho(\sigma)\bar{y}_l(\tau)\bar{y}_m(\sigma)e^{i\zeta(\tau - \sigma)},$$

where $W(\tau)$ is the dipole wake function. The use of Fourier transform of the resistive wall wake function

$$z(\omega) \stackrel{\text{def}}{=} \int_{-\infty}^{\infty} \frac{\mathrm{H}(\tau)}{\sqrt{|\tau|}} e^{i\omega\tau} \, \mathrm{d}\tau = \sqrt{\frac{\pi}{2}} \frac{1 + i \, \mathrm{sgn}(\omega)}{\sqrt{|\omega|}},$$

where $\mathrm{H}(\tau)$ is a Heaviside step function, allows to reduce double integral to a single one in a following manner:

$$\hat{W}_{lm} = \int_{-\infty}^{\infty} \int_{-\infty}^{\infty} \mathrm{d}\sigma \, \mathrm{d}\tau$$
$$\frac{\mathrm{H}(\sigma - \tau)}{\sqrt{|\sigma - \tau|}} \rho(\tau)\rho(\sigma)\bar{y}_l(\tau)\bar{y}_m(\sigma)e^{i\zeta(\tau - \sigma)}$$
$$= (-1)^m \left[\frac{1 - i}{\sqrt{2}} \int_{-\infty}^{\zeta} \frac{I_l(\omega)I_m(\omega)}{\sqrt{\zeta - \omega}} \frac{\mathrm{d}\omega}{2\sqrt{\pi}} \right.$$
$$\left. + \frac{1 + i}{\sqrt{2}} \int_{\zeta}^{\infty} \frac{I_l(\omega)I_m(\omega)}{\sqrt{\omega - \zeta}} \frac{\mathrm{d}\omega}{2\sqrt{\pi}} \right].$$

Absolute values of matrix elements of $|\hat{W}_{10 \times 10}|$ for several fixed values of ζ are plotted in Fig. 4

Detuning Wake

The matrix elements of the detuning (quadrupole) wake operator in no-wake modes basis are determined as

$$\hat{D}_{lm} = \int_{-\infty}^{\infty} \int_{\tau}^{\infty} D(\tau - \sigma)\rho(\tau)\rho(\sigma)\bar{y}_l(\tau)\bar{y}_m(\tau) \, \mathrm{d}\sigma \, \mathrm{d}\tau,$$

where $D(\tau)$ is the detuning wake function. The calculation of matrix elements can be simplified by reducing double integration via factorization of the integrand:

$$\hat{D}_{lm} = \int_{-\infty}^{\infty} \int_{-\infty}^{\infty} \mathrm{d}\sigma \, \mathrm{d}\tau$$
$$\frac{\mathrm{H}(\sigma - \tau)}{\sqrt{|\sigma - \tau|}} \rho(\tau)\rho(\sigma)\bar{y}_l(\tau)\bar{y}_m(\tau)$$
$$= \int_{-\infty}^{\infty} \mathbf{D}(\tau)\rho(\tau)\bar{y}_l(\tau)\bar{y}_m(\tau) \, \mathrm{d}\tau.$$

The function $\mathbf{D}(\tau)$ describes the wake quadrupole field along the bunch and is the same for all matrix elements:

$$\mathbf{D}(\tau) = \int_{-\infty}^{\infty} \frac{\mathrm{H}(\sigma - \tau)}{\sqrt{|\sigma - \tau|}} \rho(\sigma) \, \mathrm{d}\sigma = \int_0^{\infty} \frac{\rho(\sigma + \tau)}{\sqrt{\sigma}} \, \mathrm{d}\sigma.$$
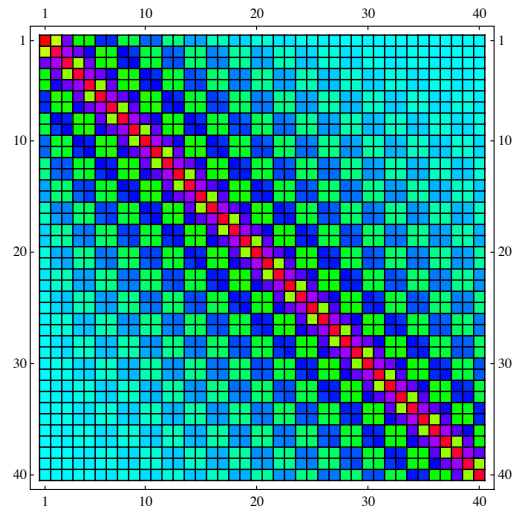

Figure 5: Values of 40 by 40 detuning resistive wall wake matrix, $\hat{D}_{lm}$.

STABILITY ANALYSIS

With the damper, the dynamic equation reads as

$$y(\tau)'' + \nu\, e^{-\tau^2/2}\, y(\tau) = \varkappa\, N\left(\hat{W} + \hat{D}\right) y(\tau) + g\, \hat{G}\, y(\tau),$$

where g is a dimensionless complex damper gain. A straightforward way to solve this equation is to search its eigenfunctions $\tilde{y}_k(\tau)$ as expanded over the no-wake basis $\bar{y}_k(\tau)$:

$$\tilde{y}(\tau) = \sum_{k=0}^{\infty} C_k\, \bar{y}_k(\tau).$$

This substitution immediately leads to the linear matrix problem for eigensystem

$$\left[\varkappa\left(\hat{W} + \hat{D}\right) + g\, \hat{G} + \text{diag}\{\nu\}\right] \mathbf{C} = \tilde{\nu}\, \mathbf{C},$$

where $\mathbf{C} = [C_0, C_1, C_2, \ldots]^T$ is a vector of coefficients C_i to be determined from eigensystem problem, and, $\text{diag}\{\nu\}_{lm}$ is a diagonal matrix $\nu_l \delta_{lm}$ whose k-th diagonal element is a k-th eigenvalue of the no-wake case.

Example 1: TMCI and Damper

With precalculated values of the wake and damper operators, coherent tunes and instabilities thresholds can be obtained using the *SCHARGEV* solver. By plotting real and imaginary parts of the eigenfrequencies one can determine the threshold of instabilities when the first mode coupling appears. Example of eigenfrequencies with and without damper usage are shown in a Fig. 6. In this particular case damping allows to move the instability threshold, which can be clearly seen from diagrams with imaginary parts. Note that first intersection of modes in the case with damper does not lead to mode coupling.
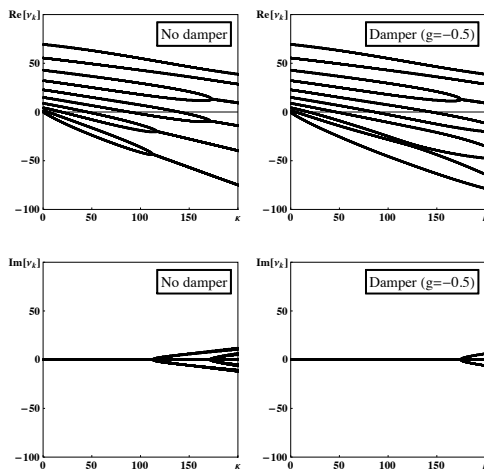

Figure 6: First ten coherent tunes of the Gaussian bunch for zero chromaticity and resistive wake as functions of wake amplitude, $\tilde{\varkappa}$. Left figures show no damper case, while right ones show eigenfrequencies for damper with gain $g = -0.5$. Real and imaginary parts are plotted at the top and bottom rows respectively.

Example 2: Fermilab Recycler

The dependence of the growth rate of the most unstable mode on the head-tail phase and damper gain for single Gaussian bunch in Fermilab Recycler obtained via *SCHARGEV* is presented in Fig. 7. Left and right figures are showing results of analysis for horizontal and vertical degrees of freedom,

$$\left[\frac{\varkappa}{2}\left(\hat{W} - \hat{D}\right) + g\, \hat{G} + \text{diag}\{\nu\}\right] \mathbf{C} = \tilde{\nu}\, \mathbf{C}$$

and

$$\left[\varkappa\left(\hat{W} + \frac{\hat{D}}{2}\right) + g\, \hat{G} + \text{diag}\{\nu\}\right] \mathbf{C} = \tilde{\nu}\, \mathbf{C}$$
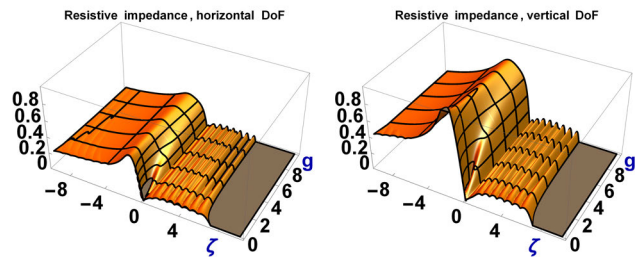
respectively.

Figure 7: Growth rate of the most unstable mode versus the head-tail phase and damper gain for Fermilab Recycler ($\kappa = 3.5$).

REFERENCES

[1] A. Burov, Phys. Rev. ST Accel. Beams 12, 044204 (2009).

[2] T. Zolkin, A. Burov, "*SCHARGEV*: Vlasov Solver for Space Charge Bunched Beams", MOPMA042, *these proceedings*, IPAC'15, Richmond, VA, USA (2015).

[3] T. Zolkin, "Beam Transverse Instability in the FNAL Booster", *Ph.D. Thesis*, The University of Chicago, Chicago, IL, USA (2014).

[4] V. Balbekov, Report No. FERMILAB-PUB-09-322 (2009).